AD-A092 938 DEFENCE RESEARCH ESTABLISHMENT OTTAWA (ONTARIO) F/G 14/2
SYSTEM SENSITIVITY ANALYSIS ACOUSTO-OPTIC SPECTRUM ANALYSIS REC--ETC(U)
FEB 80 J P LEE
UNCLASSIFIED DREO-TN-80-18 NL

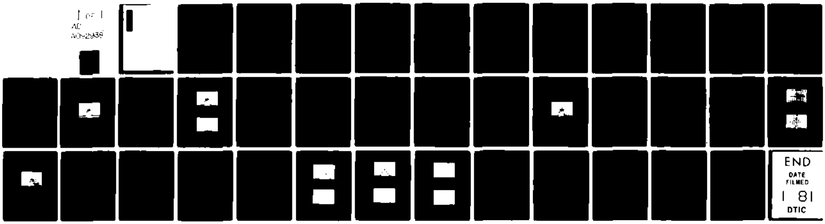

AD A092938

10

RESEARCH AND DEVELOPMENT BRANCH

DEPARTMENT OF NATIONAL DEFENCE
CANADA

14 DREO-TN-80-18

DEFENCE RESEARCH ESTABLISHMENT OTTAWA

9 TECHNICAL NOTE NO. 80-18

6 SYSTEM SENSITIVITY ANALYSIS
OF THE
ACOUSTO-OPTIC SPECTRUM ANALYSIS RECEIVER

by
10 J.P. Lee
Radar ESM Section
Defence Electronics Division

12 40

11 FEB[redacted]
OTTAWA

PROJECT NO.
31B00

404576 9 ll

ABSTRACT

This paper examines the system sensitivity of the acousto-optic spectrum analysis receiver for pulse-modulated CW signals with different pulse-widths. Considerations are given on such determining factors as the time-bandwidth product and the integration time of the photo-detector array. Measurements were taken and found to agree well with theory.

RÉSUMÉ

Le présent document étudie la sensibilité d'un récepteur d'analyse de spectre à des signaux OE à modulation par impulsion, pour différentes largeurs d'impulsion. Les facteurs déterminants dont il est tenu compte sont notamment le produit temps-largeur de bande et la durée d'intégration du réseau photodétecteur. Des mesures ont été faites; elles confirment la théorie.

TABLE OF CONTENTS

ACKNOWLEDGEMENT

The author wishes to express his sincere thanks to Mr. L.G. Rowlandson, Head, Radar ESM Section for reviewing this report and providing many valuable suggestions.

SYSTEM SENSITIVITY ANALYSIS OF THE ACOUSTO-OPTIC SPECTRUM ANALYSIS RECEIVER

1.0 INTRODUCTION

A bulk, acousto-optic, spectrum analysis receiver was designed and configured for use in a laboratory environment. This experimental receiver is being used to measure operating characteristics and the effectiveness of this technology for ESM application.

The receiver uses a bulk, Bragg cell, to provide diffraction of coherent, laser light and the subsequent formation of spectrum data on particular I.F. input signals.

Measurements were made on the sensitivity of the receiver for both pulse and CW type of signals and comparisons made with the predicted performance based on theory.

It will become evident from the material presented herein that an acousto-optic spectrum analyzer exhibits characteristics similar to a channelized receiver of equivalent bandwidth and a sensitivity also comparable to a superheterodyne receiver having equivalent frequency resolution.

2.0 THEORETICAL ANALYSIS

A schematic diagram of the acousto-optic spectrum analyzer is shown in Figure 1, where a collimated light beam impinges on the Bragg cell at the Bragg angle, θ_B. Assume the Fourier transform lens to be ideal and the amplitude weighting function given by:

$$w(y_0) = \mathrm{rect}\,(y_0/D) \qquad (1)$$

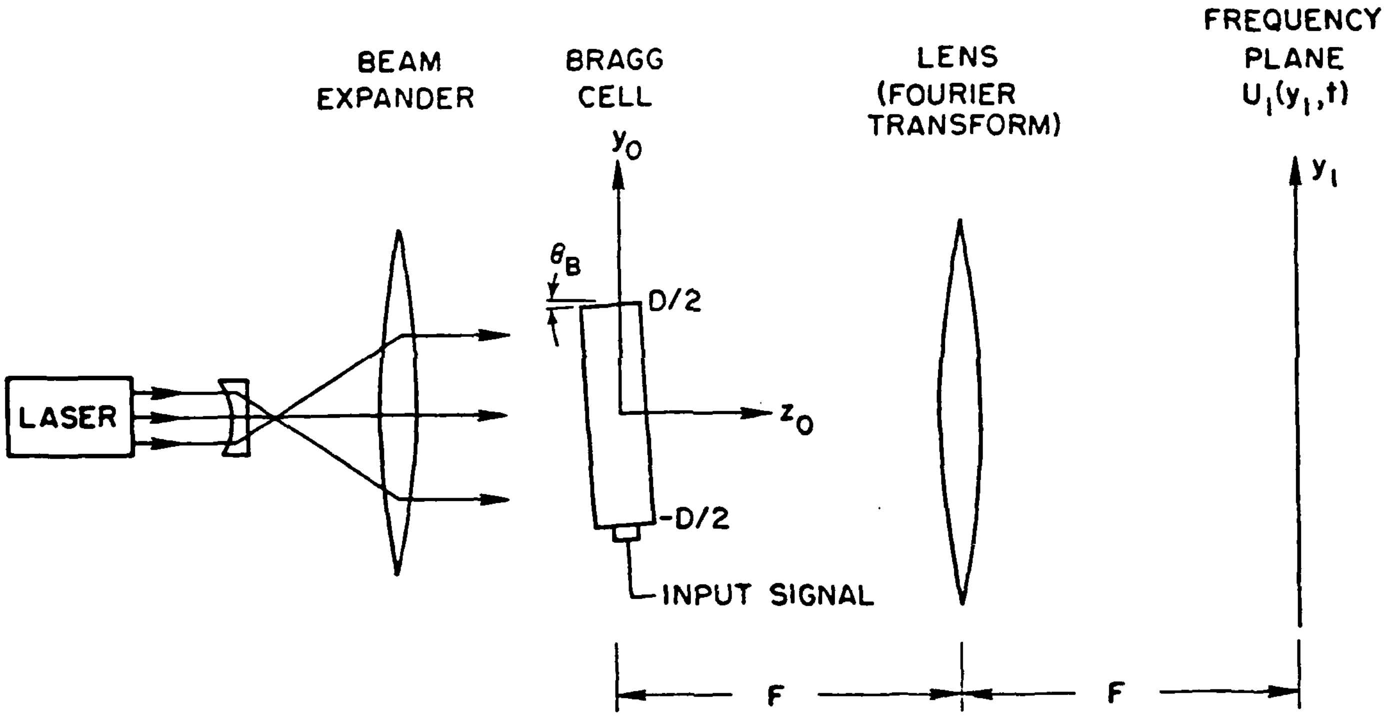

Figure 1 - SCHEMATIC DIAGRAM OF ACOUSTO-OPTIC SPECTRUM ANALYZER

The diffracted light intensity distribution at the Bragg angle in the frequency plane in one dimension for a CW signal is approximately given by (Lee):

$$|U(y_1)|^2 = \left[A \frac{\sin\left(\pi\left(\frac{y_1}{\lambda F} - \frac{f}{v_s}\right)D\right)}{\pi\left(\frac{y_1}{\lambda F} - \frac{f}{v_s}\right)} \right]^2 \tag{2}$$

where:

- f is the signal carrier frequency
- λ is the optical wavelength
- F is the focal length of the Fourier transform lens
- v_s is the acoustic wave velocity
- A is a constant

Using Rayleigh's criterion, the spot width is obtained by letting:

$$\left(\frac{y_1}{\lambda F} - \frac{f}{v_s}\right) D = 1$$

therefore:

$$y_1 = \frac{\lambda F}{D} + \frac{\lambda F}{v_s} f \tag{3}$$

where:

- $\frac{\lambda F}{v_s} f$ is the centre location of the spot
- $\frac{\lambda F}{D}$ is the width of the spot

The total displacement (y_1) of the focused beam as a function of the Bragg cell bandwidth (Δf) is obtained by using eq. (3), therefore:

$$\Delta y_1 = \frac{\lambda F}{v_s} \Delta f \tag{4}$$

The number of resolvable spots is given by:

$$\begin{aligned} N &= \frac{\text{total displacement}}{\text{spot width}} \\ &= \frac{\frac{\lambda F}{v_s} \Delta f}{\frac{\lambda F}{D}} \\ &= \frac{D \quad \Delta f}{v_s} \\ &= \tau \; \Delta f \qquad \text{(time-bandwidth product)} \end{aligned} \tag{5}$$

where:

τ is the transit time across the aperture

Δf is the bandwidth of the Bragg cell

If a CW signal and a white noise source are applied to the acousto-optic spectrum analyzer, the CW signal will form a spot in the frequency plane while the noise will spread its energy across Δy_1. The maximum signal to noise enhancement factor of the system is given by the time-bandwidth product of the Bragg cell.

For the case where a CW signal of amplitude v(t) and a gaussian noise of n(t) are applied to the acousto-optic spectrum analyzer, cross-modulation and intermodulation products may be generated. The strongest intermodulation modes which interfere spatially with the principal modes in the first diffraction order correspond to a third order interaction.

If diffraction efficiencies are constrained to approximately 1% per signal and fractional bandwidth is limited to one octave to avoid harmonic responses, then spurious free dynamic range of 50 dB can be achieved (D.L Hecht). Neglecting the small intermodulation products generated, the diffracted light intensity distribution in the frequency plane for small signal approximation, is given by:

$$|U(y_1,t)|^2 = C_1 \left(v(y_1,t) + n(y_1,t)\right)^2 \tag{6}$$

where C_1 is just a constant

If an integrating photo-detector array is used for detection in the frequency plane, the time integrated output (V_{out}) for an integration time (T) is given by:

$$V_{out} = C_1 \int_0^T \left(v(y_1,t) + n(y_1,t)\right)^2 dt$$

$$= C_1 \int_0^T v^2(y_1,t)dt + C_1 \int_0^T n^2(y_1,t)dt + 2C_1 \int_0^T v(y_1,t)n(y_1,t)dt \tag{7}$$

Where $v(y_1,t)$ and $n(y_1,t)$ are statistically independent and $n(y_1,t)$ has zero mean, therefore the third term in the above equation becomes negligible comparing to the first and second terms. Rewriting equation (7), we have:

$$V_{out} = C_1 \int_0^T v^2(y_1,t) + C_1 \int_0^T n^2(y_1,t)dt$$

$$= \text{Signal Energy} + \text{Noise Energy} \tag{8}$$

From the above equation, it is seen that the time integrated outputs of both the signal and noise are uncorrelated, and thus super-position can apply. In other words, the output signal to noise ratio is independent of the duration of the integration time of the photo-detector array.

As a result, the maximum receiver sensitivity for CW signals will only be determined by the Spatial Integration Factor which is the time-bandwidth product of the Bragg cell. In other words, the time-bandwidth product determines the maximum sensitivity which can be obtained for a given system. Therefore, it determines the maximum output to input signal to noise ratio improvement for a CW signal.

For pulses there are two effects which can reduce the maximum sensitivity which can be achieved. One is if the signal spectrum is wider than the achievable frequency resolution, that is if the pulse is shorter than τ, thereby reducing the theoretically available time-bandwidth (spatial integration effect). Another effect is if the pulse width is shorter than the integration period of the photo-detector array, the noise power will be integrated longer than the signal and thus lowering the system sensitivity.

3.0 EXPERIMENTAL MEASUREMENTS

In the experimental set-up, a Reticon photo-detector array was used with an integration time of 4 msec. The system was configured to give a frequency resolution of 1 MHz per photo-detector element. A 50 MHz bandpass filter centered at 150 MHz was placed in series with the Bragg cell. The noise produced by a travelling wave tube, RF amplifier was amplified such that other noise sources appearing on the photo-detector array became negligible.

3.1 CW Signals

The maximum theoretical signal to noise enhancement ratio should be equal to the time-bandwidth product of the Bragg cell which for an ideal rectangular bandpass filter is given by:

$$\tau\,\Delta f = 10\ \mu\text{sec} \times 50\ \text{MHz}$$

$$= 500 \qquad (9)$$

To realize this theoretically available enhancement it would be necessary to use 500 detector elements giving a frequency resolution of 0.1 MHz per element.

However, only 50 elements were used to cover the bandwidth of 50 MHz to give a resolution of 1 MHz and an effective time-bandwidth product of only 50.

Therefore, for this experiment the system could provide a maximum signal to noise ratio enhancement of 50, or 17 dB.

There are two methods in which the receiver sensitivity can be measured:

(i) Absolute minimum detectable signal power measurement: The absolute input power level is measured directly when the output signal to noise power ratio is equal to one.

(ii) Relative signal to noise enhancement ratio measurement: The output signal to noise power ratio is measured when the input signal is equal to the input noise power.

Both methods were used in the measurements and the diagram of the set-up is shown in Figure 2.

3.1.1 ABSOLUTE MINIMUM DETECTABLE SIGNAL POWER MEASUREMENT

The photo-detectors integrate the received light intensity and the output signal as a voltage is therefore equivalent to energy since photo-detection is a square law process. In turn, energy is the product of power and time.

Therefore, when using a CW signal the output signal to noise voltage ratio is equivalent to the energy ratio and is also equivalent to the power ratio of the two signals since the integration times for the CW signal and noise are equal.

Figure 3 shows the voltage output ratio from the photo-detector array for a CW signal in the presence of the amplified receiver noise. This voltage ratio represents the energy and power ratio, therefore:

$$\frac{S_0 + N_0}{S_0} = 2 \quad \text{and} \quad (S/N)_0 = 1 \tag{10}$$

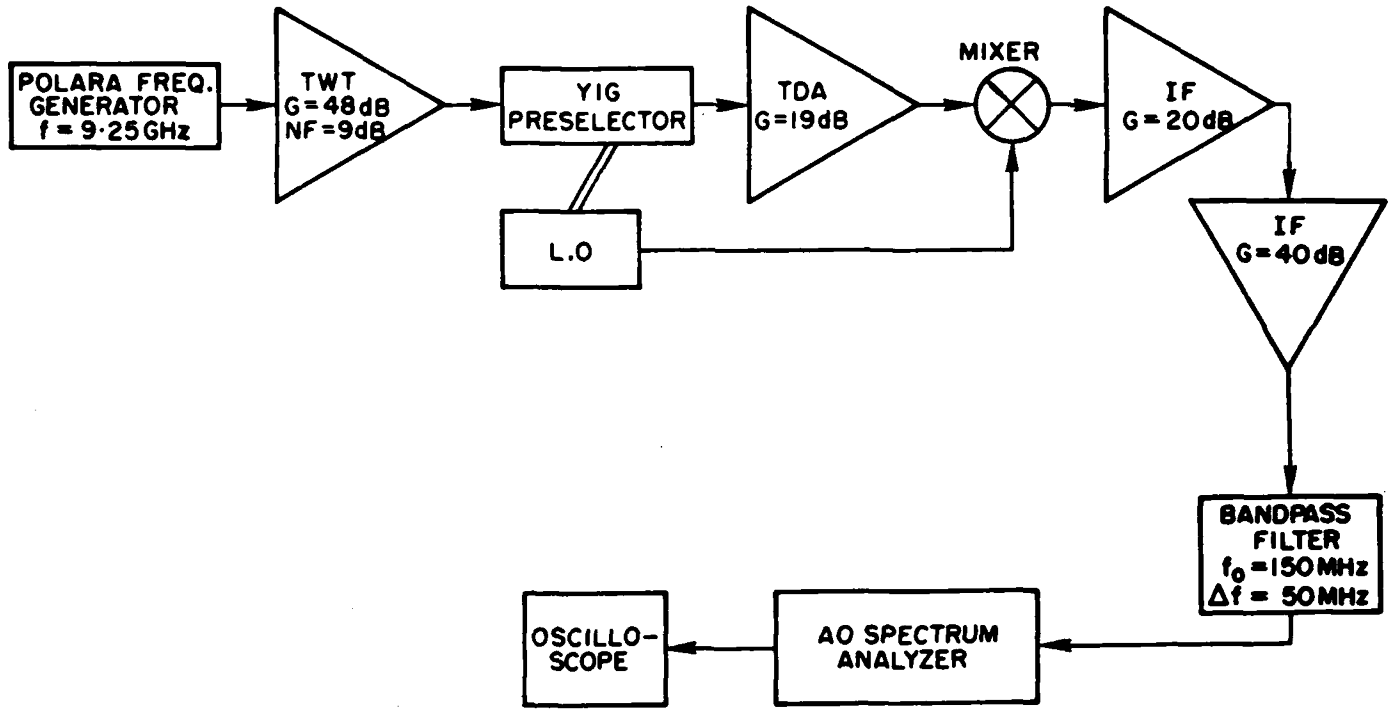

Figure 2 - SCHEMATIC DIAGRAM OF SET-UP FOR CW MEASUREMENTS

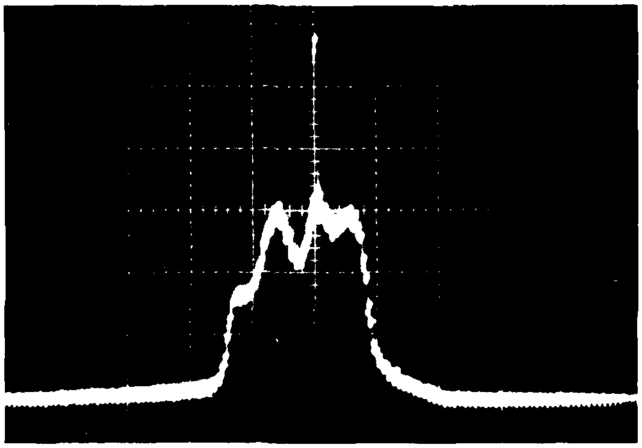

Figure 3 - OUTPUT WAVEFORM FOR THE CW SIGNAL AND NOISE WITH $(S/N)_0 = 1$ (VERTICAL SCALE: 0.2 V/D, HORIZONTAL SCALE: 0.1 msec/D, 26.88 MHz/D)

The noise power level is equal to the Boltzmann noise plus the noise figure of the input RF amplifier, which for a 1 MHz detector bandwidth is given by:

$$N = KTB + N_f$$
$$= (-114 + 9) \text{ dBm}$$
$$= -105 \text{ dBm} \tag{11}$$

where:

K = 1.38×10^{-23} Joules per deg K.

T = absolute temperature (290 ^oK)

B = effective noise bandwidth (1 MHz)

N_f = the noise figure of the RF amplifier (9 dB)

The input signal power S should then be −105 dBm, equal to the noise power, N. The input CW signal generator indicated the power to be −104 dBm which is in good agreement with the theoretical prediction.

3.1.2 Relative Signal to Noise Enhancement Ratio Measurement

The output noise level distribution with no CW signal present is shown in Figure 4. The amplitude of the noise in the photo-detector element where the test CW signal will appear is measured to be 0.60 volts. With the addition of the CW signal, the total input power measured by a power meter increased by 3 dB indicating a signal to noise ratio of unity. The combined signal and noise input power was then attenuated by 10 dB to prevent the photo-detector array from saturating. The output is shown in Figure 5 and the amplitude of the output signal is given by:

$$S_0 = 5.2 \times 0.5 \text{ volts} \times 10 = 26 \text{ volts}$$

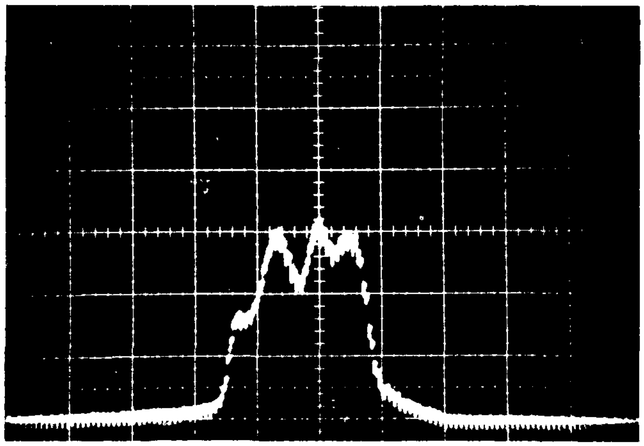

Figure 4 - OUTPUT NOISE LEVEL DISTRIBUTION (VERTICAL SCALE: 0.2 V/D, HORIZONTAL SCALE: 0.1 msec/D, 26.88 MHz/D)

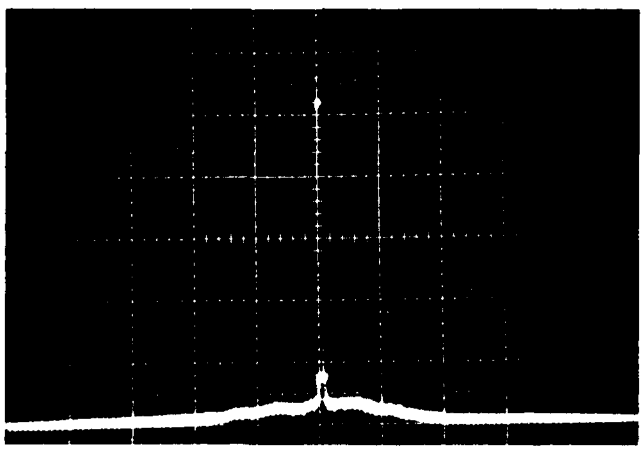

Figure 5 - OUTPUT CW AND NOISE DISTRIBUTION (VERTICAL SCALE: 0.5 V/D, HORIZONTAL SCALE: 0.1 msec/D, 26.88 MHz/D)

Since the power and energy ratio for CW is expressed by the output voltage ratio then:

$$(S/N)_0 = \frac{26 \text{ volts}}{0.60 \text{ volts}} = 43.3 = 16.4 \text{ dB} \qquad (12)$$

This value agrees very well with the theoretical value of 17 dB given in Section 3.1.

3.1.3 OUTPUT SIGNAL TO NOISE RATIO AS A FUNCTION OF INTEGRATION TIME

In the analysis given above, it was proved that the output signal to noise ratio of a CW signal was independent of the duration of the integration time of the photo-detector array. Some measurements were taken to verify the theory. An output signal to noise ratio around unity with an integration time of 4 msec was taken as a reference, then the integration time was changed and the new signal to noise ratio was recorded. The results are tabulated in Table I and plotted in Figure 6 as a function of integration time. Photographs showing the output signal and noise distributions at the various integration times are given in Appendix I. The dark current level as a function of integration time for the Reticon RL 1024 S is given in Appendix II. From the measurements, it is clear that the output signal to noise ratio of a CW signal is independent of the integration time.

In the analysis presented in this paper, the output integrated noise energy used is mainly the D.C. bias level for the long integration time considered. As given in eq. 7, there are actually two components due to the input noise; one is a D.C. bias level and the other is a A.C. noise level. If the D.C. bias level is subtracted off from the output, the processor gain due to incoherent integration can be realized. The processing gain is defined as the ratio of the input signal-to-noise without integration, to the input signal-to-noise ratio with integration in order to achieve the same detection probability. The processing gain is proportional to the square root of the integration time.

TABLE I

OUTPUT SIGNAL TO NOISE RATIO AS A

FUNCTION OF INTEGRATION TIME

INTEGRATION TIME		TOTAL SIGNAL AND NOISE POWER LEVEL (V)	NOISE POWER LEVEL (V)	SIGNAL POWER LEVEL (V)	$(S/N)_0$
ABSOLUTE (mSEC)	RELATIVE				
4	1.0	0.675	0.345	0.33	0.957
6	1.5	0.95	0.49	0.46	0.939
8	2.0	1.30	0.67	0.63	0.940
10	2.5	1.70	0.89	0.81	0.910
12	3.0	1.89	0.96	0.93	0.969
14	3.5	2.20	1.11	1.09	0.982

3.2 PULSE MODULATED SIGNALS

The experimental receiver has a time-bandwidth product of 50. With a 50 MHz bandwidth imposed on the receiver the frequency information can then be resolved to 1 MHz.

The period of integration was set by the frame time of 4 ms. That is, the charge or energy accumulated by each detector was sampled every 4 ms and the charge removed in this process. This means that for signals having a duration longer than 4 ms, such as CW, the maximum sensitivity is realized and is equal to the value given by the CW signal experiment by Section 3.1.1, namely about -104 dBm.

For pulsed signals less than 4 ms and greater than 1 μsec in length, the sensivivity is reduced in proportion to the pulse width/4 ms. The system sensitivity for a pulse can then be related to the CW signal sensitivity.

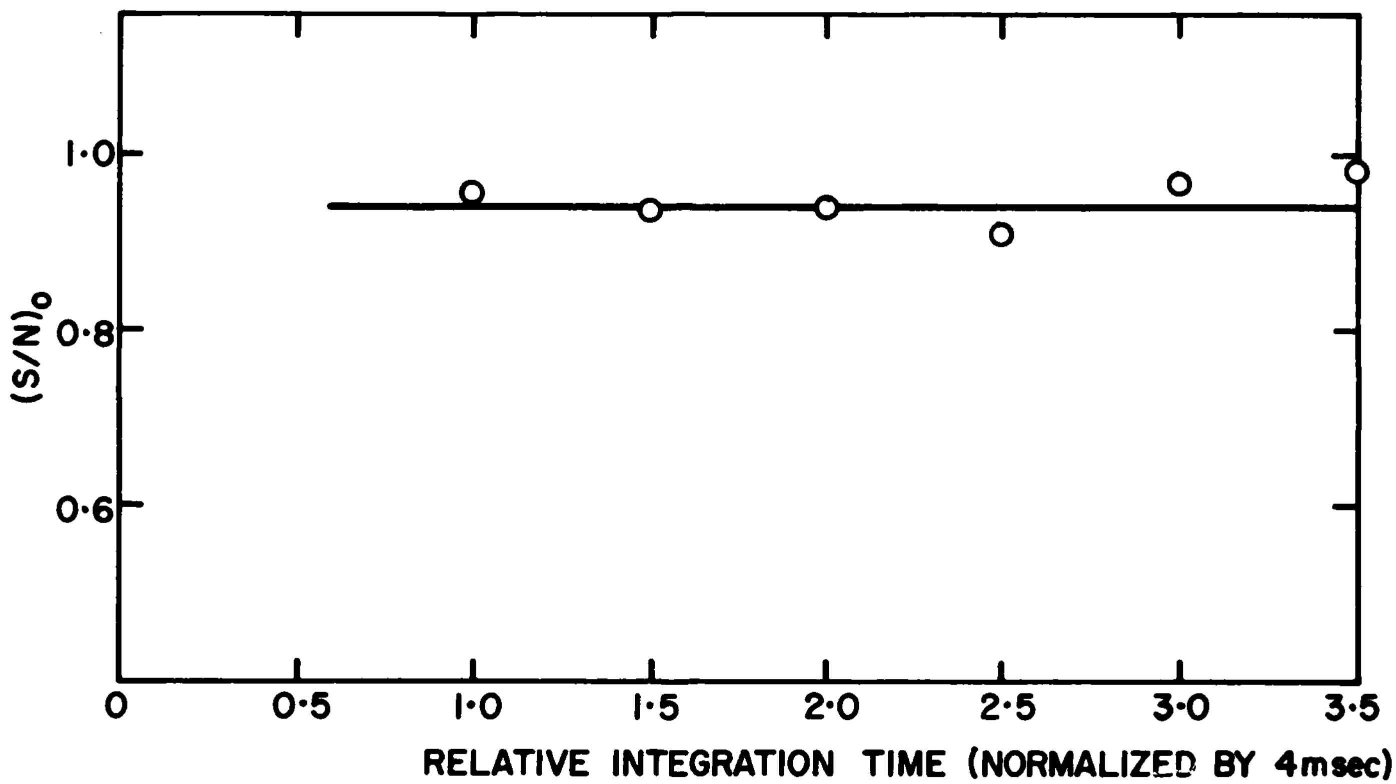

Figure 6 - OUTPUT SIGNAL TO NOISE RATIO FOR A CW SIGNAL AS A FUNCTION OF INTEGRATION TIME

For example, using a 10 μsec pulse, the sensitivity reduction is given by:

$$\frac{\text{Pulse energy detected}}{\text{CW energy detected}} = \frac{10 \text{ sec}}{4 \text{ ms}}$$

$$= -26 \text{ dB} \tag{13}$$

Therefore, in effect, the pulse power would have to be increased by 26 dB to achieve the same signal voltage output as a CW at the end of a 4 ms frame (integration period). In other words, the receiver sensitivity for $(S/N)_0$ of unity using a 10 μsec pulse is then about -79 dBm.

An experiment was carried out for different pulse widths to demonstrate this effect. Figure 7 shows the experimental set-up. A CW signal at 9.25 GHz was chosen as the reference and measurements were made of the additional pulse power required to equal the CW signal output for a $(S/N)_0$ of unity.

Figure 8 shows the output signal to noise conditions for $(S/N)_0$ equal to unity for a 50% duty cycle CW signal. The difference in the pulse and CW power to achieve this output for different pulse widths was recorded from the calibrated microwave signal generator.

Results are shown in Table II for pulse widths down to 2 μsec. Theoretical values are also given which show good agreement with the experimental values.

It should be noted that the sensitivity of the receiver to pulsed signals is falling in proportion to the decrease in pulse width. For example, a pulse width reduction from 100 to 50 μsec, a factor of 2, causes about a 3 dB loss in sensitivity.

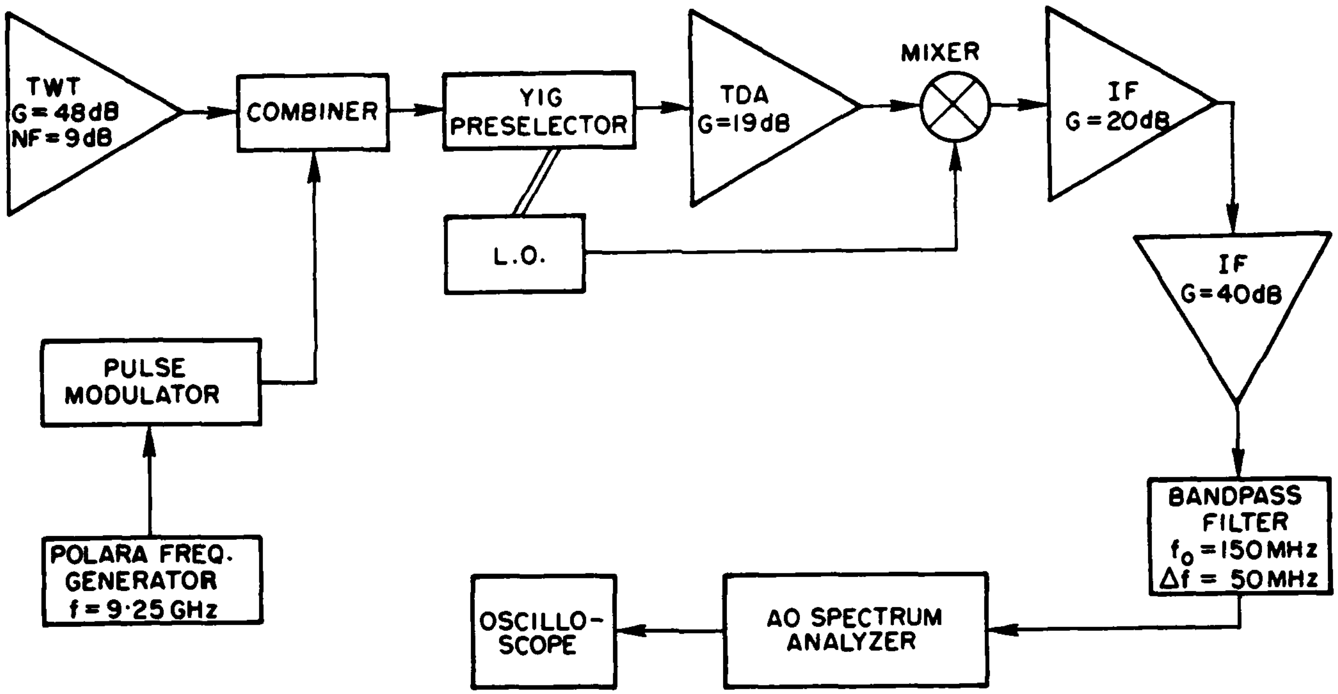

Figure 7 - SCHEMATIC DIAGRAM OF SET-UP FOR PULSE MEASUREMENTS

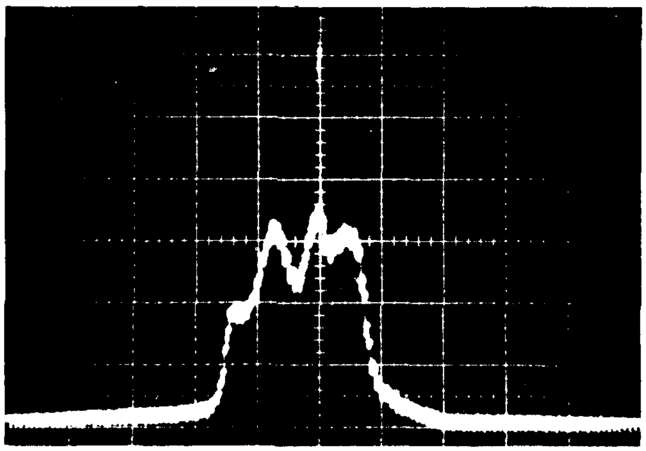

Figure 8 - OUTPUT WAVEFORM DISTRIBUTION FOR A 50% DUTY CYCLE CW AND NOISE WITH $(S/N)_0 = 1$ (VERTICAL SCALE: 0.2 V/D, HORIZONTAL SCALE: 0.1 msec/D, 26.88 MHz/D)

TABLE II

SENSITIVITY MEASUREMENTS FOR PULSES GREATER THAN ONE μSEC

PULSE WIDTH (μSEC)	INPUT POWER READING (dBm)	INCREASE IN INPUT POWER LEVEL RELATIVE TO A CW SIGNAL, TO GIVE SAME OUTPUT $(S/N)_0 = 1$ (dB)	
		THEORETICAL	EXPERIMENTAL
2	-27.8	33.0	34.2
5	-33.5	29.0	28.5
10	-36.5	26.0	25.5
30	-40.0	21.3	22.0
50	-42.8	19.0	19.2
80	-44.8	17.0	17.2
100	-46.2	16.0	15.8

From Table II, it is apparent that there is good agreement between the predicted and experimental results.

The effect of pulse width reduction was discussed at the beginning of this section and it was stated that for pulse widths less than the integration period the detected energy fell in proportion to the reduction in pulse width.

Referring to equation (5), the maximum gain-bandwidth achievable by the reciever is 500, and only 50 is achieved for the experimental system because 50 detector elements rather than 500 were used. From the gain-bandwidth product available of 50 and using a 50 MHz bandwidth the frequency resolution achievable is 1 MHz with 50 detectors. Since the frequency resolution is proportioned to $1/\tau$, the effective transit time is reduced to 1 μsec.

Providing the pulse width remains longer than 1 μsec the spectral energy is essentially contained within a 1 MHz bandwidth and most of the energy can be captured by one detector. When the pulse width becomes less than 1 μsec the energy extends beyond 1 MHz with a resultant decrease in sensitivity referred to the single detector in question. The results given in Table I show the effect of this spatial integration factor.

So for pulse widths decreasing below 1 μsec the receiver sensitivity degrades in proportion to the amount the pulse width is less than 1 μsec. For example, for a 0.1 μsec pulse the reduction in sensitivity is 10 dB less than for a 1 μsec pulse due to spectral broadening. Coupled with a 10 dB reduction due to reduced integration time the net effect is a 20 dB degradation in sensitivity in going from 1 μsec to 0.1 μsec pulse width.

An experiment was carried out using pulse widths much less than those reported in Table II. The method of relative comparison with a CW signal was used to measure the degradation in sensitivity. Two hundred and five pulses within a 4 ms frame were used in order to lower the peak power applied to the Bragg cell.

Table III shows the results of this experiment. For a single pulse of width less than 1 μsec the loss in sensitivity is now greater than was produced earlier (Table II) by only the time integration effects. For example, for a 0.5 μsec pulse the loss from 1 μsec is 6 dB or a factor of 4, combining a factor of 2 for reduced integration time and a factor of 2 for spectral broadening.

TABLE III

SENSITIVITY MEASUREMENTS FOR PULSES LESS THAN ONE μSEC

PULSE WIDTH (μSEC)	INPUT POWER READING (dBm)	INCREASE IN INPUT POWER LEVEL, RELATIVE TO A CW SIGNAL TO GIVE SAME OUTPUT, $(S/N)_0 = 1$ (dB)		
		THEORETICAL (SINGLE PULSE)	EXPERIMENTAL	
			205 PULSES	SINGLE PULSE
1.0	-24.0	36.0	14.0	37.1
0.8	-22.0	38.0	16.0	39.1
0.7	-21.2	39.1	16.8	39.9
0.5	-18.8	42.0	19.2	42.3
0.4	-16.8	44.0	21.2	44.3
0.3	-14.8	46.5	23.2	46.3
0.2	-10.5	50.0	27.5	50.6

Figure 9 (a), (b) and (c) show oscilloscope records of the spectral distribution and amplitude of pulse modulated CW signals.

TABLE IV

THEORETICAL AND EXPERIMENTAL SINGLE PULSE SENSITIVITY

FOR INTEGRATING PHOTODETECTOR ARRAY

PULSE WIDTH (μSEC)	INPUT POWER LEVEL TO GIVE $(S/N)_0 = 1$ (dBm)	
	THEORETICAL	EXPERIMENTAL
0.2	-64.0	-62.4
0.3	-67.5	-66.7
0.4	-70.0	-68.7
0.5	-72.0	-70.7
0.7	-74.9	-73.1
0.8	-76.1	-73.9
1.0	-78.0	-75.9
2.0	-81.0	-78.8
5.0	-85.0	-84.5
10.0	-88.0	-87.5
30.0	-92.8	-91.0
50.0	-95.0	-93.8
80.0	-97.0	-95.8
100.0	-98.0	-97.2
CW	-114.0	-113.0

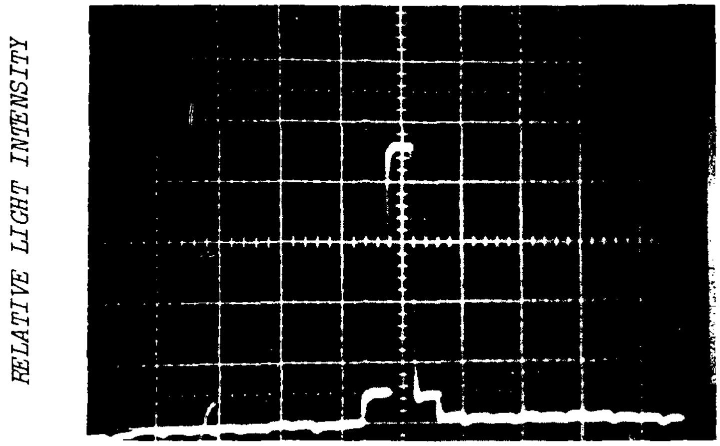

Figure 9(a) - PULSE WIDTH = 100 μSEC

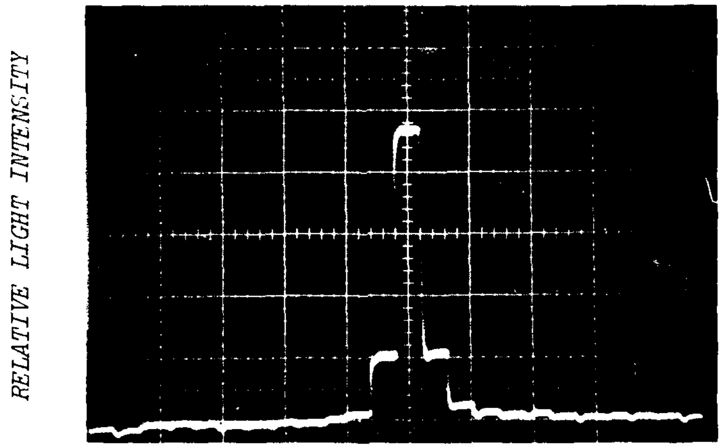

Figure 9(b) - PULSE WIDTH = 1 μSEC

Figure 9 - OUTPUT WAVEFORM DISTRIBUTIONS FOR PULSE MODULATED CW SIGNALS AT VARIOUS PULSE WIDTHS (VERTICAL SCALE: 0.5 V/D, HORIZONTAL SCALE: 10 μSEC/D, 2.7 MHz/D)

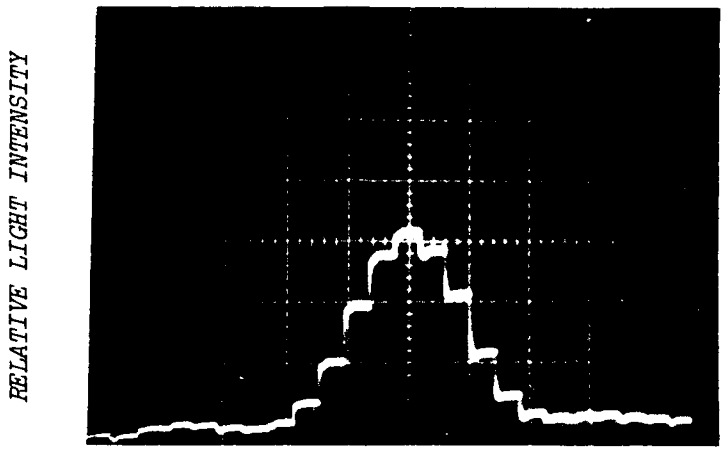

Figure 9(c) - PULSE WIDTH = 0.2 μSEC

Figure 9 - OUTPUT WAVEFORM DISTRIBUTIONS FOR PULSE MODULATED CW SIGNALS AT VARIOUS PULSE WIDTHS (VERTICAL SCALE: 0.5 V/D, HORIZONTAL SCALE: 10 μSEC/D, 2.7 MHz/D)

4.0 SUMMARY OF THEORETICAL AND EXPERIMENTAL RESULTS FOR CW AND PULSE SIGNALS

Table IV compiles the information obtained from experiments and theoretical predictions for a single pulse and CW.

The effects of pulse width and spectral broadening can best be seen by referring to Figure 10.

For CW and pulses longer than 4 ms the receiver sensitivity is normalized to -114 dBm which excludes the noise factor, N_f, of the RF amplifier. One may then adjust the curve for any given N_f thereby making the results shown here more useful.

For pulse widths less than 4 ms the receiver sensitivity degrades at a rate of 3 dB per octave reduction in pulse width due to decreased integration.

For pulse widths less than 1 μsec a further degradation of 3 dB/octave occurs due to spectral broadening for a combined effect of 6 dB/octave.

5.0 SIGNIFICANCE OF RESULTS FROM ESM APPLICATION OF AO RECEIVER

In Radar ESM applications, the types of signals intercepted are usually of very short duration over a wide power range.

The acousto-optic spectrum receiver employing an integrating photo-detector array is an energy detection system and thus signals of equal average power will give about the same output level when integrated over a relatively long time.

The receiver sensitivity for pulse signals is determined by two contributing factors, namely the spatial integration factor and the time integration factor due to the integrating photo-detector array. Noise is present continuously and as a result, the output noise increases linearly with the integration period. For a fixed system configuration with a certain noise bandwidth, the sensitivity for short pulses improves with shorter integration time since less noise energy is integrated.

If a photo-detector array responds only to peak powers, the signal output would be essentially independent of the time integration factor and only the spatial integration factor would contribute to the resultant sensitivity of the receiver. Current efforts are aimed at achieving this through development of a peak detecting array exhibiting the electrical equivalent of a "sample and hold" circuit characteristic.

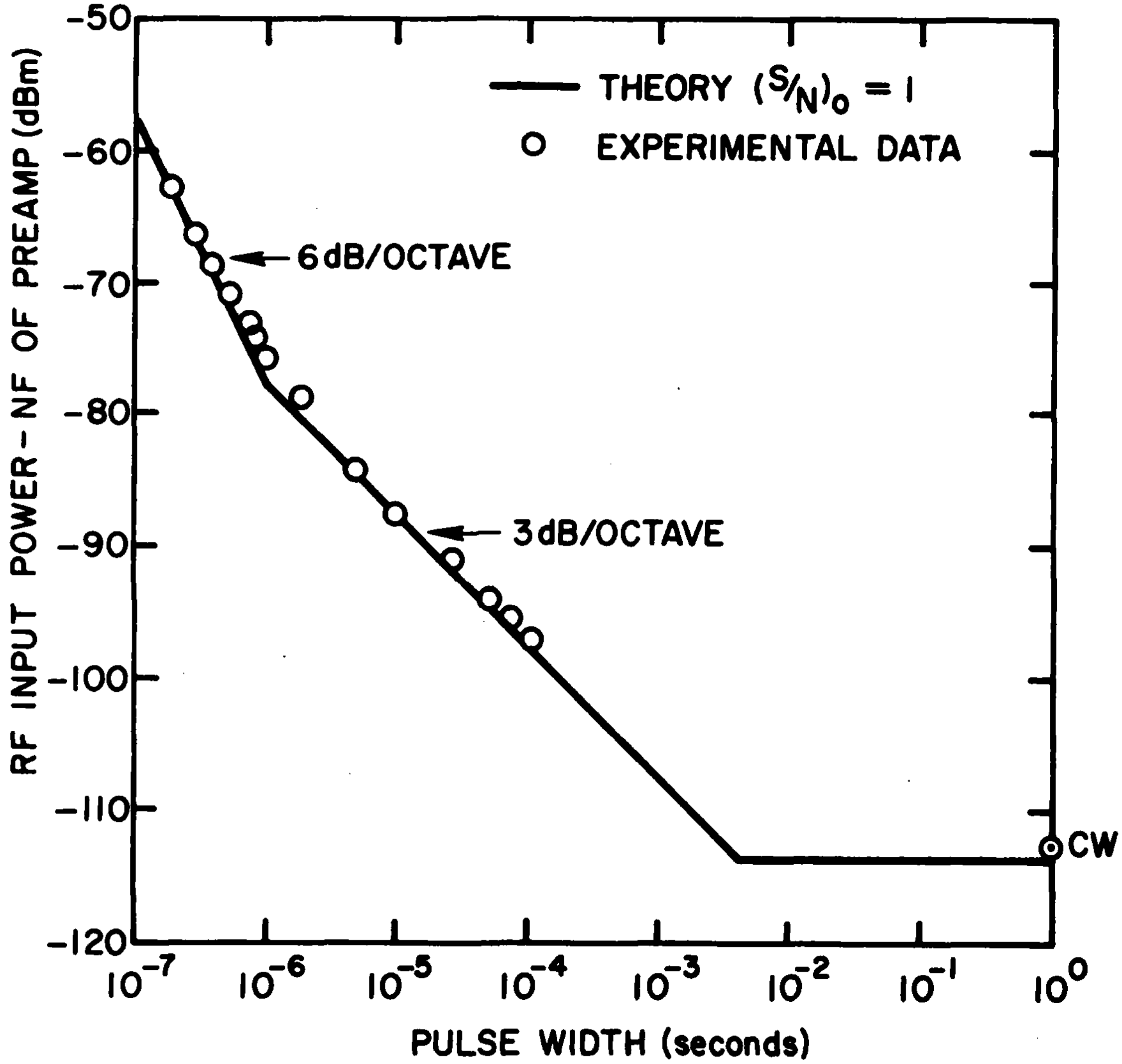

FIGURE 10 - THEORETICAL AND EXPERIMENTAL SINGLE PULSE SENSITIVITY FOR INTEGRATING PHOTODETECTOR ARRAY (1 Mhz/ELEMENT, INTEGRATION TIME = 4 msec)

6.0 REFERENCES

1. J.P. Lee, "Signal Analysis using the Acousto-Optic Spectrum Analyzer", Technical Note No. 80-2. RESM, DND, Canada, November 1979.

2. D.L. Hecht, "Spectrum Analysis Using Acousto-Optic Devices", Optical Engineering, Vol. 16, No. 5, Sept./Oct. 1977, pp. 461-466.

APPENDIX I

OUTPUT SIGNAL AND NOISE DISTRIBUTIONS AT VARIOUS INTEGRATION TIMES

The following photographs show the signal and noise distributions for a CW signal at various integration times.

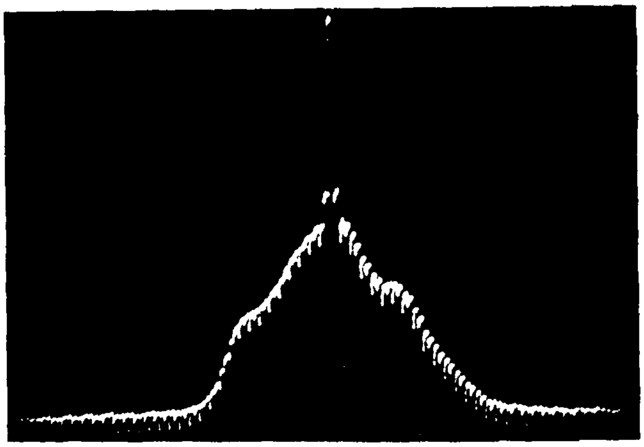

(a) INTEGRATION TIME = 4 msec
VERTICAL SCALE: 0.1 V/D

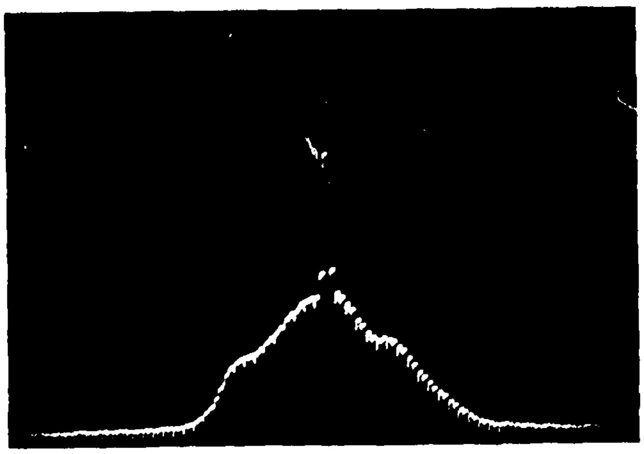

(b) INTEGRATION TIME = 6 msec
VERTICAL SCALE: 0.2 V/D

Figure I-1 OUTPUT SIGNAL AND NOISE DISTRIBUTIONS AS A FUNCTION OF INTEGRATION TIME, HORIZONTAL SCALE: 50 μSEC/D

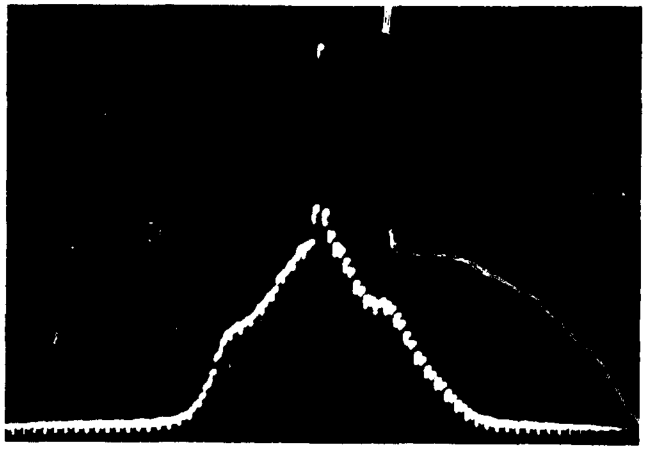

(a) INTEGRATION TIME = 8 msec
VERTICAL SCALE: 0.2 V/D

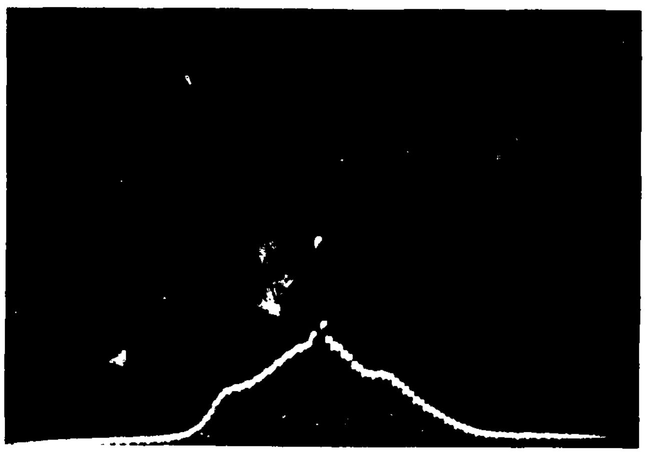

(b) INTEGRATION TIME = 10 msec
VERTICAL SCALE: 0.5 V/D

Figure I-2 OUTPUT SIGNAL AND NOUSE DISTRIBUTIONS AS A FUNCTION OF INTEGRATION TIME, HORIZONTAL SCALE: 50 μSEC/D

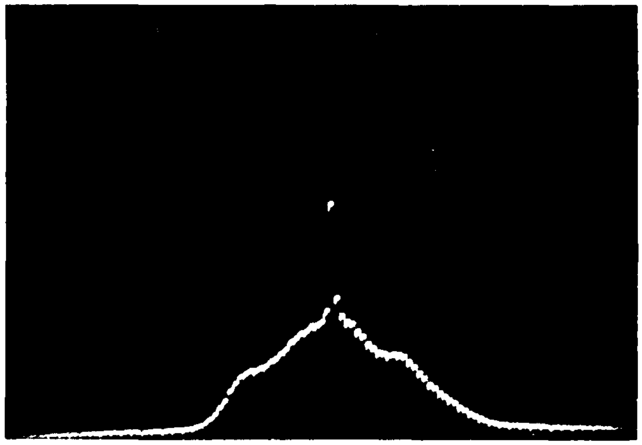

(a) INTEGRATION TIME = 12 msec
VERTICAL SCALE: 0.5 V/D

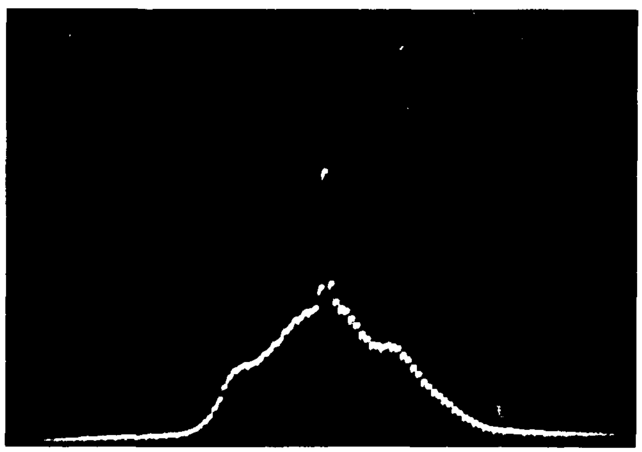

(b) INTEGRATION TIME = 14 msec
VERTICAL SCALE: 0.5 V/D

Figure I-3 OUTPUT SIGNAL AND NOISE DISTRIBUTIONS AS A FUNCTION OF INTEGRATION TIME, HORIZONTAL SCALE: 50 μSEC/D

APPENDIX II

DARK CURRENT LEVEL VERSUS INTEGRATION TIME

FOR THE RETICON RL 1024 S

The measurements were taken by operating the photo-detector array in room temperature and in complete darkness. The results are tabulated in Table II-I and plotted in Figure II-1. From the plot, it is seen that the dark current level increases directly proportional to the integration time. By extending the line to the vertical axis, it shows that there is an offset of about 35 mv in the circuitry.

TABLE II-1

DARK CURRENT LEVEL VERSUS INTEGRATION TIME

INTEGRATION TIME (m SEC)	OUTPUT LEVEL (mV)
4	37.5
6	45.0
8	53.5
10	59.0
12	65.0
14	69.0
16	74.0
18	79.0
20	84.0
22	89.0
24	92.0
26	96.0
28	100.5
30	104.0
32	110.0

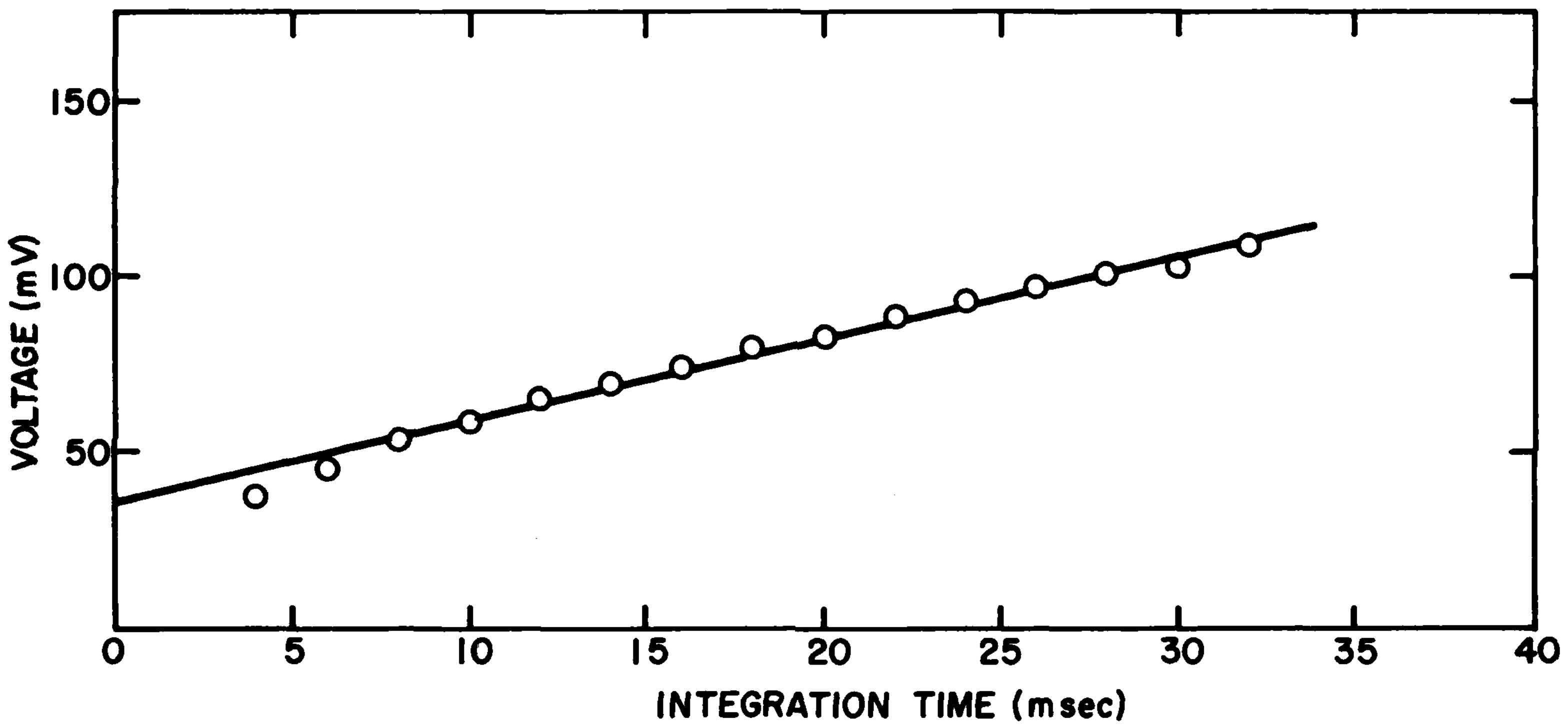

FIGURE II-1 DARK CURRENT LEVEL VERSUS INTEGRATION TIME FOR THE RETICON RL 1024 S (V_{SAT} = 3 V)

UNCLASSIFIED

Security Classification

DOCUMENT CONTROL DATA – R & D

(Security classification of title, body of abstract and indexing annotation must be entered when the overall document is classified)

1 ORIGINATING ACTIVITY Defence Research Establishment Ottawa National Defence Headquarters Ottawa Ontario, Canada, K1A 0Z4	2a. DOCUMENT SECURITY CLASSIFICATION Unclassified
	2b GROUP IV

3 DOCUMENT TITLE

SYSTEM SENSITIVITY ANALYSIS OF THE ACOUSTO-OPTIC SPECTRUM ANALYSIS RECEIVER

4 DESCRIPTIVE NOTES (Type of report and inclusive dates)

Technical Note

5 AUTHOR(S) (Last name, first name, middle initial)

LEE J.P.

6 DOCUMENT DATE FEB 1980	7a. TOTAL NO OF PAGES 41	7b NO. OF REFS 2

8a. PROJECT OR GRANT NO 31B00	9a. ORIGINATOR'S DOCUMENT NUMBER(S) DREO TN 80- 18
8b CONTRACT NO	9b. OTHER DOCUMENT NO.(S) (Any other numbers that may be assigned this document)

10 DISTRIBUTION STATEMENT

Qualified requesters may obtain copies of this document from their defence documentation center.

11 SUPPLEMENTARY NOTES	12. SPONSORING ACTIVITY CRAD

13 ABSTRACT

This paper examines the system sensitivity of the acousto-optic spectrum analysis receiver for pulse-modulated CW signals with different pulse-widths. Considerations are given on such determining factors as the time-bandwidth product and the integration time of the photo-detector array. Measurements were taken and found to agree well with theory.

DSIS

77-06

Security Classification

KEY WORDS

ACOUSTO-OPTICS

ESM RECEIVER

SIGNAL TO NOISE RATIO IMPROVEMENT

INSTRUCTIONS

1. ORIGINATING ACTIVITY: Enter the name and address of the organization issuing the document.

2a. DOCUMENT SECURITY CLASSIFICATION: Enter the overall security classification of the document including special warning terms whenever applicable.

2b. GROUP: Enter security reclassification group number. The three groups are defined in Appendix 'M' of the DRB Security Regulations.

3. DOCUMENT TITLE: Enter the complete document title in all capital letters. Titles in all cases should be unclassified. If a sufficiently descriptive title cannot be selected without classification, show title classification with the usual one-capital-letter abbreviation in parentheses immediately following the title.

4. DESCRIPTIVE NOTES: Enter the category of document, e.g. technical report, technical note or technical letter. If appropriate, enter the type of document, e.g. interim, progress, summary, annual or final. Give the inclusive dates when a specific reporting period is covered.

5. AUTHOR(S): Enter the name(s) of author(s) as shown on or in the document. Enter last name, first name, middle initial. If military, show rank. The name of the principal author is an absolute minimum requirement.

6. DOCUMENT DATE: Enter the date (month, year) of Establishment approval for publication of the document.

7a. TOTAL NUMBER OF PAGES: The total page count should follow normal pagination procedures, i.e., enter the number of pages containing information.

7b. NUMBER OF REFERENCES: Enter the total number of references cited in the document.

8a. PROJECT OR GRANT NUMBER: If appropriate, enter the applicable research and development project or grant number under which the document was written.

8b. CONTRACT NUMBER: If appropriate, enter the applicable number under which the document was written.

9a. ORIGINATOR'S DOCUMENT NUMBER(S): Enter the official document number by which the document will be identified and controlled by the originating activity. This number must be unique to this document.

9b. OTHER DOCUMENT NUMBER(S): If the document has been assigned any other document numbers (either by the originator or by the sponsor), also enter this number(s).

10. DISTRIBUTION STATEMENT: Enter any limitations on further dissemination of the document, other than those imposed by security classification, using standard statements such as:

(1) "Qualified requesters may obtain copies of this document from their defence documentation center."

(2) "Announcement and dissemination of this document is not authorized without prior approval from originating activity."

11. SUPPLEMENTARY NOTES: Use for additional explanatory notes.

12. SPONSORING ACTIVITY: Enter the name of the departmental project office or laboratory sponsoring the research and development. Include address.

13. ABSTRACT: Enter an abstract giving a brief and factual summary of the document, even though it may also appear elsewhere in the body of the document itself. It is highly desirable that the abstract of classified documents be unclassified. Each paragraph of the abstract shall end with an indication of the security classification of the information in the paragraph (unless the document itself is unclassified) represented as (TS), (S), (C), (R), or (U).

The length of the abstract should be limited to 20 single-spaced standard typewritten lines; 7½ inches long.

14. KEY WORDS: Key words are technically meaningful terms or short phrases that characterize a document and could be helpful in cataloging the document. Key words should be selected so that no security classification is required. Identifiers, such as equipment model designation, trade name, military project code name, geographic location, may be used as key words but will be followed by an indication of technical context.

DATE
ILMED

8